BIO-OPTICS FOR OCEAN COLOR REMOTE SENSING

OF THE BLACK SEA

(Black Sea Color)

TN 14: Algorithm development

Workpackage:	*4*	
Author(s):	*V. Slabakova*	*IO-BAS*

Introduction

Satellite ocean color has given another dimension to marine biogeochemistry and ecosystem studies, offering new opportunities for direct monitoring of biodiversity and shelf - sea fronts providing key information for instance on the timing and spatial distribution of plankton blooms, the magnitude of primary production and provision of environmental data layers crucial for building predictive models of species (fish and other pelagic animals) and habitat distributions, relevant for the implementation of important EU environmental policies (Water Framework Directive, Marine Strategy Framework Directive) and climate change projections. In fact operational satellite products generally rely on algorithms developed for global applications which are the source of large uncertainties in the marginal seas. More specifically in the Black Sea, Sancak et al., 2005, Oguz, & Ediger, 2006, Suslin et al., 2018, Slabakova et al., 2011, 2020 demonstrated that the standard algorithms lead to a significant overestimation of the satellite ocean color products (on the order of hundred percent for chlorophyll a). These observed biases in retrieval of concentration of seawater optically significant constituents can have a strong impact in the use of satellite ocean color products in primary production models, in validation and tuning of ecosystem modeling and especially in the Black Sea data assimilation systems. Regional bio optical algorithms could provide a suitable solution to overcome the above problems. Kopelevich et al., 2013 and Suslin et al., 2016 showed the possibility of minimizing the uncertainties in satellite derived products by developing regional empirical and semi analytical algorithms for the Black Sea. However, the small number of measurements and the restricted number of measured seawater bio-optical quantities prevent any further development.

By far the most widely used type of bio-optical algorithms are those classified as band-ratio, empirical algorithms. Empirical algorithms do not require a full understanding of fundamental bio-optical theory. They provide a direct link between satellite-sensed radiance and relevant bio-optical parameters such as Chlorophyll a (CHL), Total Suspended Matter (TSM), Diffuse Attenuation Coefficient (K_d) and absorption by Colored Dissolved Organic Matter (CDOM) on global and regional scales (O'Reilly et al., 1998, Mueller, 2000, Tassan, 1993, Zibordi et al., 2015). The creation of empirical algorithms, however, requires a sufficient size of highly accurate field measurements with adequate spatial coverage for the regions of interest. Thus, empirical algorithms are subject to updates as the data set increases in its temporal and spatial coverage and size. The main uncertainty of empirical bio-optical algorithms includes: the respective contributions of the optically significant components; the varying relationships between the inherent optical properties (a and b_b) and the corresponding concentrations of optically active components (CHL, TSM, CDOM). However, these algorithms are the simplest and better suited to environmental monitoring which needs quick results for decision-making, therefore the empirical approaches can be easily implemented at local/regional scale.

The objective of this report is to present the development of regional bio-optical algorithms on the basis of reference bio-optical data set collected in the western Black Sea during the Bio-Opt 2019. Additionally, in the analyses are included the available bio-optical data collected in the Bulgarian Black Sea waters in the period 2011 - 2016 during different scientific initiatives using the same instruments and methods described in deliverables TN#3, 8 and 9.

2. Regional empirical algorithm for Chlorophyll *a* retrial from OLCI data

Phytoplankton are a critical component of the Earth's system. Absorbing incoming solar radiation, CO_2 and synthesizing organic matter, they are responsible for half of the planetary primary production (Longhurst et al., 1995) modulate oceanic carbon, and provide energy for the majority of marine life. A common measure of phytoplankton biomass is the chlorophyll-a (CHL) concentration the major photosynthetic pigment in marine phytoplankton.

The regional CHL algorithm was derived from the bio-optical data set (the number of data sets, N= 186) which contains coincident *in situ* remote sensing reflectance, R_{rs} (λ), and *in situ* CHL, measurements collected during bio–optical cruises in the western Black Sea (details of data measuring and processing protocols were provided in deliverables TN# 3, 8 and 9 of the project). *In situ* CHL data covered a range of 0.1–9.77 mg.m^{-3}(Tab. 1).

Table 1. Ranges of CHL (mg.m^{-3}) with median, mean, standard deviation (SD) and number of observations (N)

Parameter	Unit	Range	Median	Mean	SD	N
CHL	mg.m^{-3}	0.1-9.77	0.35	0.95	1.43	186

The regional CHL algorithm was developed by using the remote sensing reflectance (R_{rs}) ratio at 443, 490, 510 to 560 nm against CHL. The combination of band reflectance ratios from *in situ* R_{rs} data that scored the highest coefficient of determination and lower RMS error was chosen for the final algorithm.

Correlation matrices were computed for the log-transformed *in situ* data ($\log_{10}$ (CHL) vs. $\log_{10}(R_{rs}(\lambda_i)/R_{rs}(\lambda_j))$, where the λ_i is 443, 490 and 510 nm; λj= 560 nm. The corresponding regressions make use of only 2 wavelengths. The rationale for log-transforming bio-optical data relies on the log-normal distribution of seawater optical properties and concentrations of optically significant constituents over several order of magnitude (Campbell, 1995).

The relationship of log-transformed *in situ* chlorophyll concentration as a function of remote sensing reflectance ratios 443/560, 490/560, and 510/560 are presented in Figure 1. The highest correlation was obtained between the log-transformed ratio of $R_{rs}(490)/R_{rs}(560)$, and the log-transformed CHL (coefficient of determination R^2=0.88). The algorithms predict CHL values using a cubic polynomial formulation. The coefficients derived from the regression of *in situ* CHL and R_{rs} ratios are provided in Table 2.

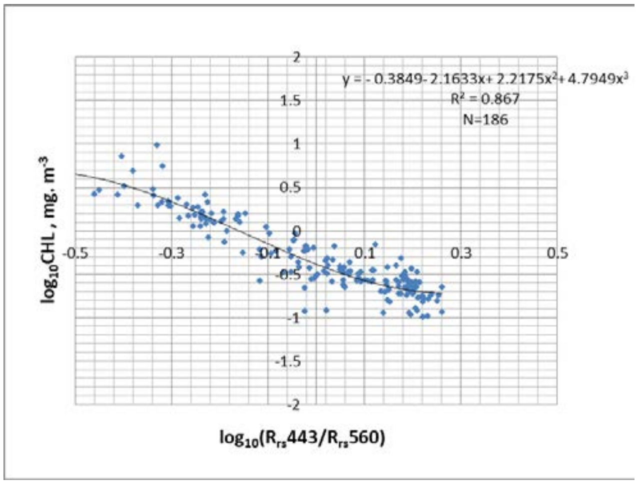

A)

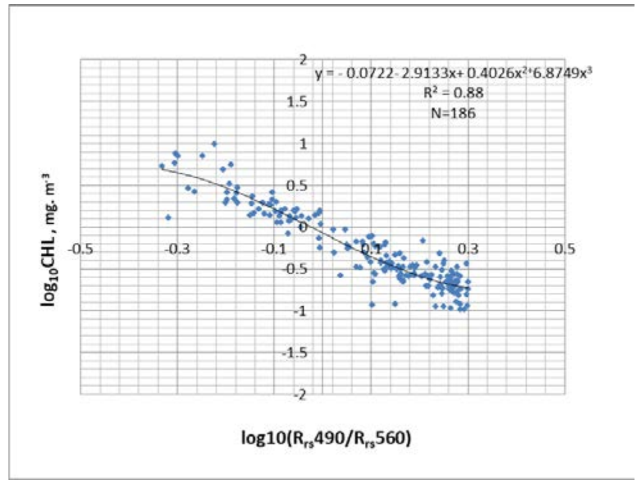

B)

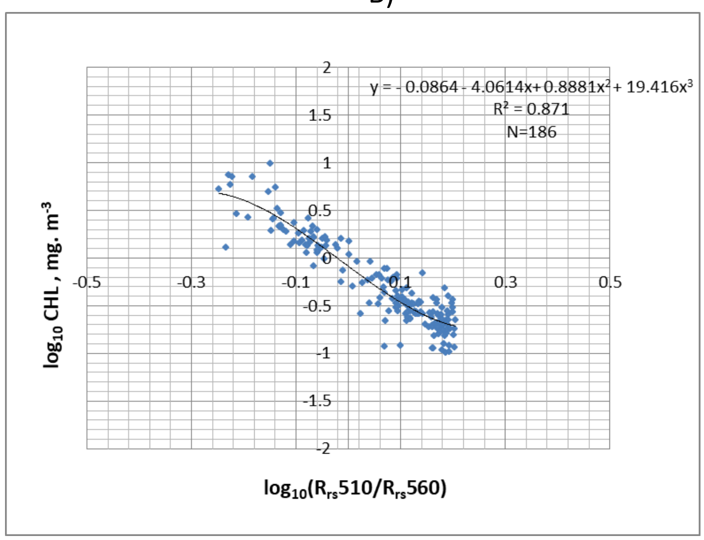

C)

Figure 1. Plot of the log-transformed *in situ* CHL concentration versus ratios of *in situ* measured: a) R_{rs} (443)/R_{rs} (560), b) R_{rs} (490) /Rrs (560) and c) R_{rs} (510) /R_{rs} (560)

Table 2. Coefficients of polynomial function $\log_{10}$(CHL)=f ($\log_{10}$(Rrs(λ_i)/Rrs(λ_j)). where the λ_i is 443, 490 and 510 nm; λ_j= 560 nm

Algorithm	a_0	a_1	a_2	a_3
R_{rs}443/R_{rs}560	-0.3849	-2.1633	2.2175	4.7949
R_{rs}490/R_{rs}560	-0.0722	-2.9133	0.4026	6.8749
R_{rs}510/R_{rs}560	-0.0864	-4.0614	0.8881	19.416

Furthermore, our bio-optical datasets were used to derive a set of coefficients for a new regional algorithm based on the standard OC4 functional form (O'Reilly et al., 1998). The standard OLCI Level 2 OC4ME algorithm (Morel et al., 2007a) makes use of the maximum band ratio between reflectances among either 443, 490, or 510, and reflectance at 560 nm, combined to a power polynomial fit of CHL concentration (in logarithm) as recalled below from (Antoine, 2010).

$$log_{10}(CHL) = a_0 + \sum_{n=1}^{N} a_i\,(MBR)^n$$

where

$$MBR = max\left[log10\left[\frac{R_{rs}(443)}{R_{rs}(560)};\frac{R_{rs}(490)}{R_{rs}(560)};\frac{R_{rs}(510)}{R_{rs}(560)}\right]\right]$$

The new coefficients were estimated through a fourth order polynomial regression between log-transformed *in situ* MBR and CHL with coefficient of determination R^2=0.88 (Fig.2).

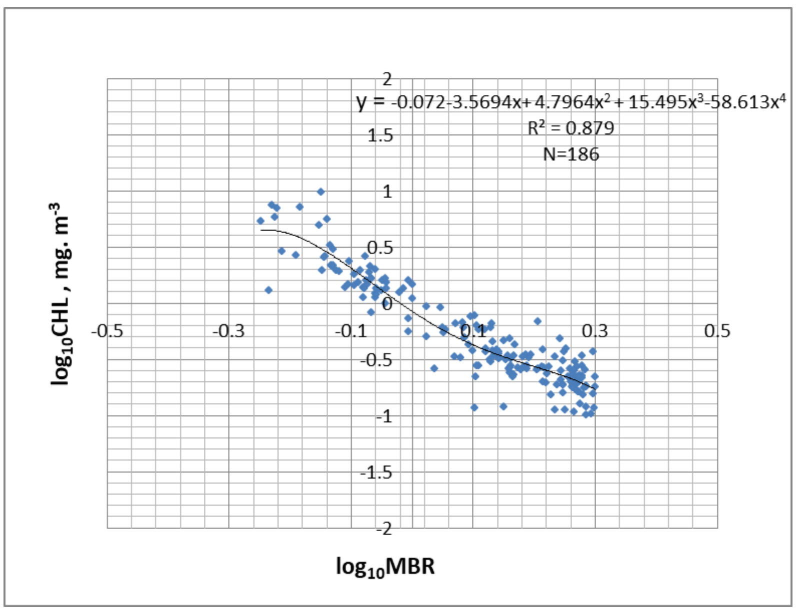

Figure 2. Relation between *in situ* MBR and CHL used to derive the new set of coefficients for the OC4ME algorithm for the Black Sea.

$$CHL_{OC4ME\_BS} = 10^{(-0.072-3.5694x+4.7964x^2+15.495x^3-58.613x^4)}$$

where $$x = max\left[log10\left[\frac{R_{rs}(443)}{R_{rs}(560)};\frac{R_{rs}(490)}{R_{rs}(560)};\frac{R_{rs}(510)}{R_{rs}(560)}\right]\right]$$

The results of comparison between estimated CHL values from 2 band ratio and MBR algorithms and *in situ* CHL are summarized in Table 3, while the scatter plots for each algorithm versus *in situ* CHL are presented in Figure 3.

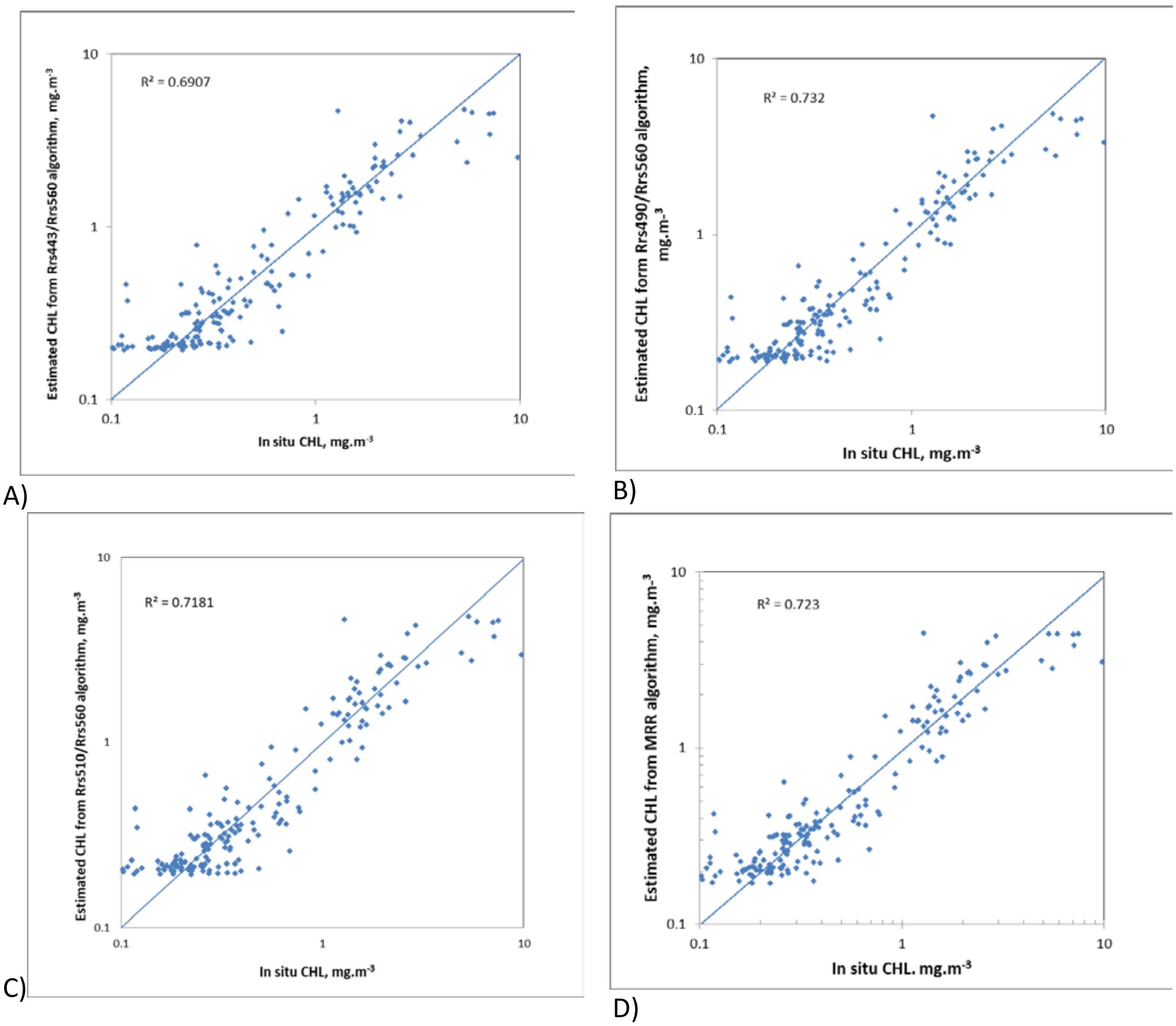

Figure 3. Scatter plots of estimated CHL values from 2 band ratio and MBR algorithms versus *in situ* CHL. A) *in situ* CHL vs R_{rs} (443)/R_{rs} (560) algorithms-retrieved CHL; B) *in situ* CHL vs R_{rs} (490)/R_{rs} (560) algorithms-retrieved CHL; C) *in situ* CHL vs R_{rs}510/R_{rs}560 algorithms-retrieved CHL;D) *in situ* CHL vs MBR algorithms-retrieved CHL

Table 3. Statistical parameters (mean percentage difference - MDP, mean absolute percentage difference-MPD, root mean square error – RMSE and coefficient of determination – R^2) estimated between *in situ* and algorithms-retrieved CHL.

Algorithm	MPD,%	MAPD,%	RMSE,	R^2

			mg.m^{-3}	
$R_{rs}443/R_{rs}560$	-7.31	29.17	0.16	0.69
$R_{rs}490/R_{rs}560$	7.09	28.82	0.15	0.73
$R_{rs}510/R_{rs}560$	7.57	30.31	0.16	0.72
MBR	7.07	29.24	0.16	0.72

The lowest corelation (R^2=0.69) between *in situ* CHL and algorithms-retrieved data was found for R_{rs} (443)/R_{rs}(560)algorithm. The highest MAPD of 30.31% was estimated for R_{rs}(510)/R_{rs}(560) algorithm. ***The best estimation of CHL values were obtained from the R_{rs}(490)/R_{rs}(560) band ratio algorithm (named BS_CHL) for which the highest coefficient of determination (R^2=0.73) and the lowest MAPD and RMS errors (correspondingly 28.82% and 0.15 mg.m^{-3}) were determined.*** The MBR algorithm is slightly inferior in comparison to R_{rs}(490)/R_{rs}(560) band ratio algorithm (R^2=0.72, MDP= 29.24% and RMSE=0.16 mg.m^{-3}).

3. Regional empirical algorithm for Total Suspended Matter (TSM) retrieval from OLCI data

The Total Suspended Matter concentration in marine waters is also an indicator of interest and can be related to water turbidity. Obviously, chlorophyll *a* and other pigments (phytoplankton) are included in this component but their corresponding concentrations only contribute for a very small amount to the TSM concentration. The optimal wavelength used to retrieve TSM depends strongly on the turbidity of the water. In general NIR bands are appropriate for higher TSM concentrations, whereas visible bands are appropriate for lower TSM concentrations. In the NIR band the turbidity of the water should be sufficiently high so that particle scattering overcomes the strong water absorption in this region.

The regional TSM algorithm was derived from the bio-optical data set (the number of data sets, N= 124) which contains coincident *in situ* remote sensing reflectance, R_{rs} (λ), and *in situ* TSM [mg/l], measurements collected during bio-optical cruises in the western Black Sea (details of data measuring and processing protocols were provided in deliverables TN# 3, 8 and 9 of the project). *In situ* TSM data covered a range of 0.19–2.61 mg/l, with average value of 0.83 mg/l (Tab. 4).

Table 4. Ranges of TSM (mg/l) with median, mean, standard deviation (SD) and number of observations (N)

Parameter	Unit	Range	Median	Mean	SD	N
TSM	mg/l	0.19-2.61	0.53	0.83	0.61	124

We derived several algorithms in different forms based on the regression of log-transformed *in situ* TSM concentrations and band ratio of remote sensing reflectance at different wavelengths. After several tests, we found the highest correlation between *in situ* $\log_{10}$(TSM) and log-transformed ratio of $R_{rs}(510)/R_{rs}(665)$, with a value of 0.85 (Fig. 4). Such ratio was also observed to provide the best estimation of TSM in the Baltic and Adriatic Seas (Berthon et al., 2006). The coefficients of the algorithm were estimated through a fourth power polynomial regression fit between log-transformed *in situ* TSM concentrations and remote sensing reflectance ratio at 510 and 665 nm.

$$TSM = 10^{(2.3865-12.922x+29.117x^2-27.995x^3+9.1924x^4)}$$

where $$x = \left[log10\left[\frac{R_{rs}(510)}{R_{rs}(665)}\right]\right]$$

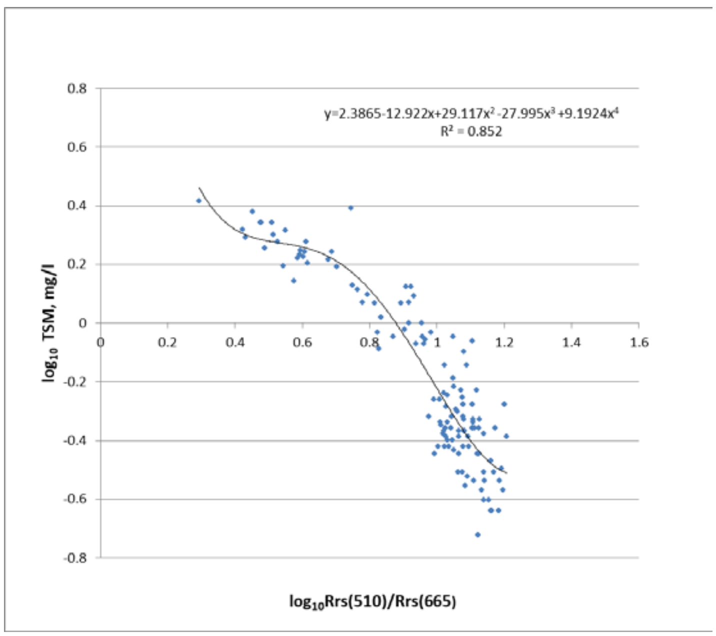

Figure 4. Plot of the log-transformed *in situ* TSM concentration versus ratio of remote-sensing reflectance at 510 and 665 nm

The comparison between *in situ* TSM concentrations and algorithm-retrieved TSM data shows that the functional form fits well the observed values (R^2=0.90) (Fig. 5). The data points are uniformly distributed around the line of best agreement. The estimated RMS is 0.11 mg/l and MAPD is 20.73%.

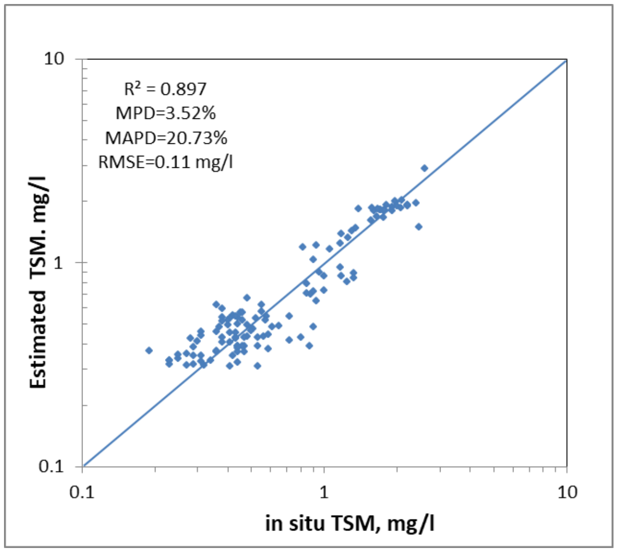

Figure 5. Scatter plot of algorithm derived TSM values *in situ* measured TSM concentrations

4. Regional empirical algorithms for absorption coefficient by *non-pigmented particles* and colored dissolved organic matter at 443 nm (ADG 443 nm) retrieval from OLCI data

The absorption coefficient ADG 443 represents the fraction of incident light absorbed by both detrital particles and colored dissolved organic matter (CDOM). Dissolved organic matter is an important component of the oceanic carbon cycle. It is also used as proxy to assess the impact of terrigenous inputs in coastal waters.

The regional ADG algorithm was derived from the bio-optical data set (the number of data sets, N= 125) which contains coincident *in situ* remote sensing reflectance, R_{rs}, and *in situ* absorption coefficients of non-pigmented a_{dt} and yellow substance measurements collected during bio-optical cruises in the western Black Sea (details of data measuring and processing protocols were provided in deliverables TN# 3, 8 and 9 of the project). *In situ* ADG at 443nm data covered a range of 0.0537 – 0.2776 m^{-1}, with average value of 0.12 m^{-1} (Tab. 6).

Table 6. Ranges of ADG (m^{-1}) with median, mean, standard deviation (SD) and number of observations (N)

Parameter	Unit	Range	Median	Mean	SD	N
ADG443	m^{-1}	0.0537-0.2776	0.103	0.12	0.005	125

The ADG at 443 was regressed against several combinations of different $R_{rs}(\lambda)$ and ratios of $R_{rs}(\lambda)$. After a number of tests, we obtained the highest correlation (R^2= 0.87) from liner regression of *in* *situ* log_{10}(ADG443) and log-transformed ratio of remote sensing reflectance at 443 and 560 nm. The relationship between *in situ* log_{10}(ADG) and $log_{10}(R_{rs}443/R_{rs}560)$ is presented in Fig. 6.

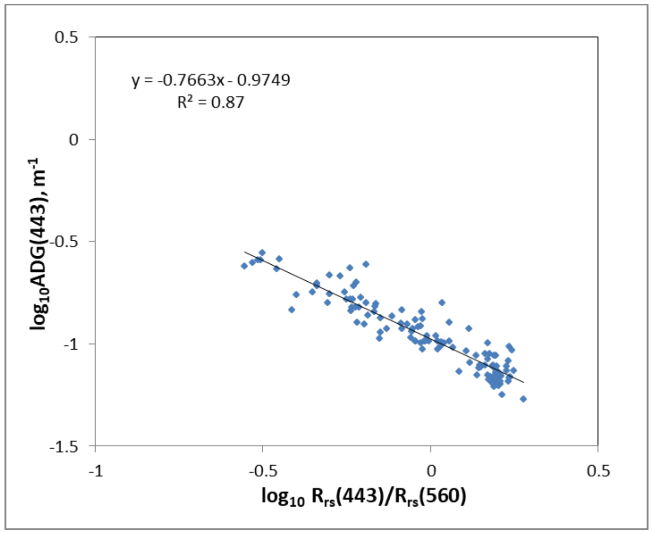

Figure 6. Plot of the log-transformed *in situ* ADG443 versus ratio of remote-sensing reflectance at 443 and 560 nm

The comparison between *in situ* ADG443 and algorithm-retrieved ADG443 values shows that the data points are uniformly distributed around the line of best agreement (R^2=0.86) (Fig. 7). The RMS is 0.06 m^{-1} and MAPD is 10.63%.

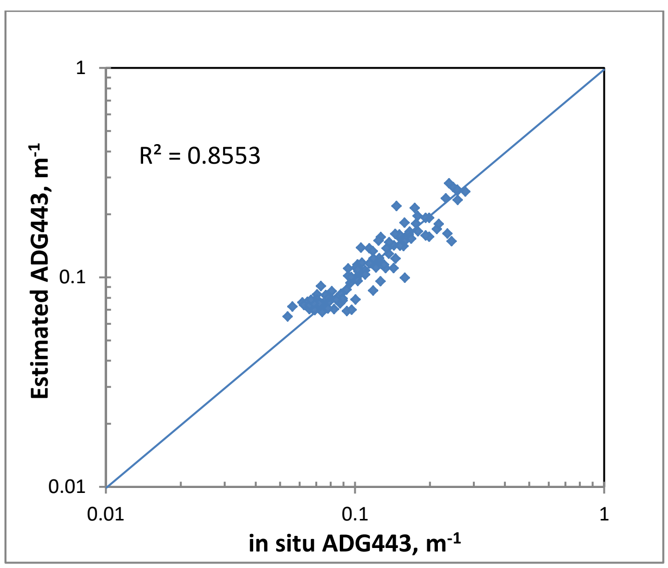

Figure 7. Scatter plot of algorithm derived ADG 443 values *in situ* measured ADG 443

5. Regional empirical algorithms for the diffuse attenuation coefficient (K_d) retrieval from OLCI data

Diffuse attenuation coefficient is one indicator of the turbidity of the water column. The global K_d (490) algorithm, suggested for the OLCI is a “OK2-560” algorithm proposed by Morel et al. (2007b). It is based on the 490/560 nm reflectance ratio, and has the form:

$$K_d(490) = 0.0166 + 10^{\sum_{x=0}^{n} A_x \left(log_{10}\left(\frac{\rho_{490}}{\rho_{560}}\right)\right)^x}$$

where 0.0166 m^{-1} is a constant value of “pure” water”, ρ490/ρ560 is the ratio of the normalized water-leaving reflectance at 490 and 560nm,and the n+1=5 coefficients has the following values: A_0= -0,82789; A_1= -1,64219; A_2=0,90261;A_3=-1,62685; A_4=0,088504

We use our bio-optical dataset to derive a new set of coefficients based on the OLCI “OK2-560” functional form. The bio-optical data contains coincident *in situ* remote sensing reflectance, R_{rs} (λ), and K_d (490) measurements collected during bio-optical cruises in the western Black Sea. The number of data sets used to statistically tune the polynomial coefficients of the “OK2-560” algorithm is 120. *In situ* K_d at 490 nm data covered a range of 0.05537– 0.83726 m^{-1} (Tab. 7).

Table 7. Ranges of K_d (490) (m^{-1}) with median, mean, standard deviation (SD) and number of observations (N)

Parameter	Unit	Range	Median	Mean	SD	N
K_d (490)	m^{-1}	0.0554–0.8373	0.1285	0.1838	0.149	120

The new coefficients were estimated through a fourth power polynomial regression fit between log-transformed *in situ* K_d (490) to ratio of remote sensing reflectance at 490 and 560 nm (Fig. 8):

$$Kd(490) = 0.0166 + 10^{(-0.6631-1.5611x-0.7827x^2+0.3631x^3+12.411x^4)}$$

where x=$log_{10}(R_{rs}490/R_{rs}560)$

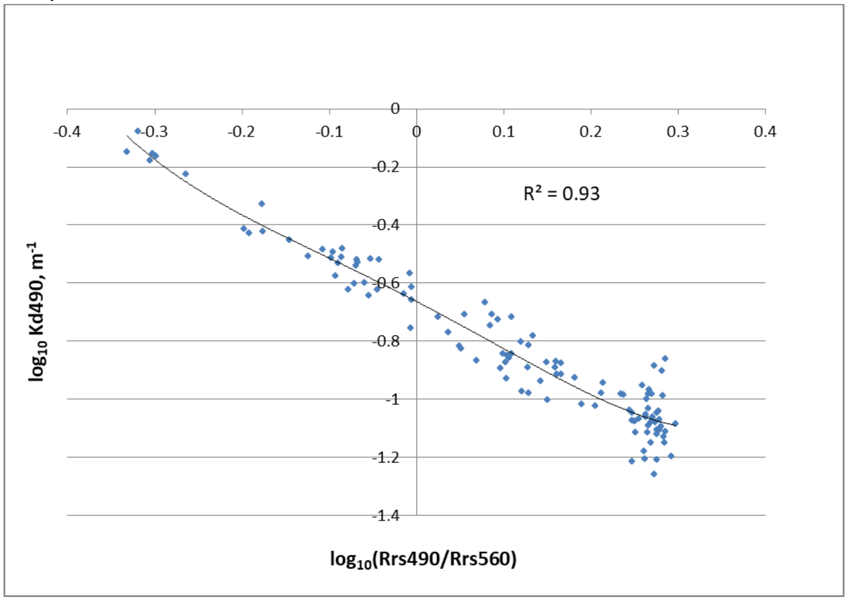

Figure 8. Plot of the log-transformed *in situ* K_d (490) versus ratio of remote-sensing reflectance at 490 and 560 nm

In Figure 9, the comparison of in situ K_d (490) and algorithm-estimated K_d (490) values shows a good agreement between data sets (R^2=0.97). The estimated RMS is 0.07 m^{-1} and MAPD is 18.42%.

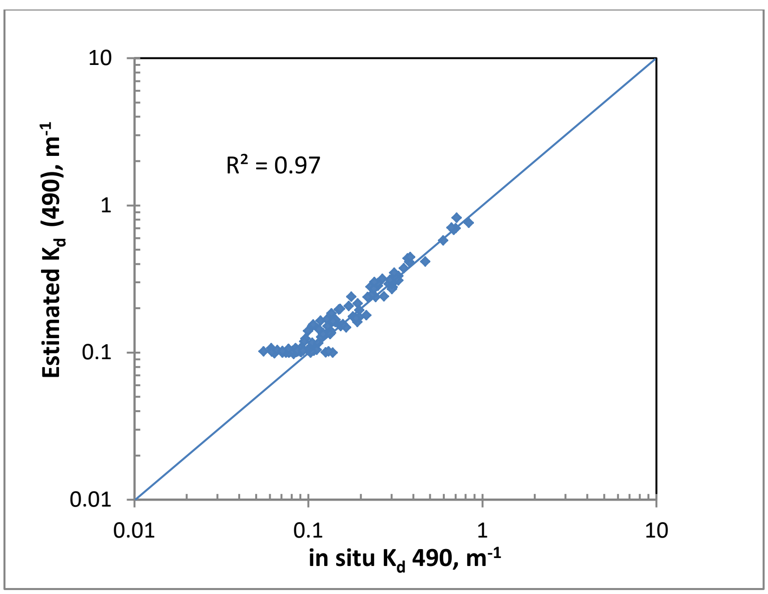

Figure 9. Scatter plot of algorithm derived K_d(490) values *in situ* measured K_d(490)

6. Conclusions

Empirical algorithms based on remote sensing reflectance band ratio are among the most simple approaches designed to retrieve the seawater optically active constituent from satellite observations. The practical utility of the method results from this simplicity. Estimates of remote sensing reflectance ratio from satellite sensors are readily available and the computation required to convert reflectance values into estimates of seawater optically constituent is straightforward and easily implemented. We have attempted to develop empirical ocean-color algorithms to retrieve the bio-optical variables CHL, TSM, ADG 443 and K_d 490 using an *in situ* bio-optical datasets collected in the western Black Sea. However, the validity of the reported empirical algorithms obviously depends on the size of the dataset used for their development. The Black Sea waters vary at a basin level due to the subregional features, environmental factors and seasonal variability, consequently the reported regional algorithms might have a limited generalization capability.

ACKNOWLEDGMENT

We would like to express our sincere thanks to Dr. Giuseppe Zibordi for providing his assistance with the processing of AOP data used in this report as well as for his continued support and Dr. Jean–Francois Berthon providing us the IOP data.

7. References:

Antoine, D. OLCI Level 2 Algorithm Theoretical Basis Document: Ocean Colour Products in Case 1 Waters; Ref S3-L2-SD-03-C10-LOVATBD. 2010. Available online: https://www.eumetsat.int/website/home/Satellites/CurrentSatellites/Sentinel3/OceanColourServices/index.html

Berthon J-F., Zibordi G., Vanderlinde D., Canuti E.,Develi E.(2006) Regional bio-optical relationships and algorithms for the Adriatic Sea, the Baltic Sea and the English Channel/North Sea suitable for ocean colour sensors , Publication of EC, 2006 , ISSN 1018-5593

Campbell, J. (1995). The Lognormal Distribution as a Model for Bio-Optical Variability in the Sea. Journal of Geophysical Research: Oceans 100 (C7), 13237–54.

Deliverable #TN3: Bio-optical cruise report, 2019.

Deliverable # TN8: Analyses and QA of AOP and IOP data, 2020

Deliverable #TN9: Analysis and QA of biological data

Kopelevich O. V., Sheberstov S. V., Sahling I. V., Vazyulya S. V., Burenkov V. I.,2013,Bio-optical characteristics of the Barents, White, Black,and Caspianseas from data of satellite ocean color scanners, http://optics.ocean.ru

Longhurst A., Sathyendranath S., Platt T., Caverhill C. (1995). An estimate of global primary production in the ocean from satellite radiometer data. J. Plankt. Res. 17, 1245–1271. 10.1093

Morel, A., Gentili, B., Claustre, H., Babin, M., Bricaud, A., Ras, J., et al. (2007a).Optical properties of the "clearest" natural waters. Limnology and Oceanography, 52, 217-229.

Morel, A., Huot, Y., Gentili, B., Werdell, P.J., Hooker, S.B. and B.A. Franz (2007b). Examining the consistency of products derived from various ocean color sensors in open ocean (Case 1) waters in the perspective of a multi-sensor approach. Remote Sensing of Environment, 111, 69-88

Mueller, J. L., (2000). SeaWiFS algorithm for the diffuse attenuation coefficient, K (490), using water-leaving radiances at 490 and 555 nm, in SeaWiFS Postlaunch Calibration and Validation Analyses, Part 3, vol. 11, edited by S. B. Hooker, and E. R. Firestone, Rep. NASA/TM-2000–206892, pp. 24–27, NASA Goddard Space Flight Cent, Greenbelt, Md.

Oguz, T. & Ediger, D. (2006). Comparison of in situ and satellite-derived chlorophyll pigment concentrations, and impact of phytoplankton bloom on the suboxic layer structure in the western Black Sea during May–June 2001. Deep Sea Res.II, 53, 1923-1933.

O'Reilly, J. E., Maritorena, S., Mitchell, B. G., Siegel,D. A., Carder, K. L., Garver, A., et al. (1998).Ocean color algorithms for SeaWiFS. Journal of Geophysical Research, 103, 24937-24953.

Tassan,S. (1993). An improved in-water algorithm for the determination of chlorophylland suspended sediment concentration from Thematic Mapper data in coastalwaters.International Journal of Remote Sensing,14(6), 1221−1229.

Sancak, T., Besiktepe, A., Lee, M., & Frouin, R. (2005) Evaluation of SeaWiFS chlorophyll-a in the Black and Mediterranean Sea. International Journal of Remote Sensing, 26, 2045-2060.

Slabakova, V., Slabakova, N., Hristova, O., & Dzhurova, B. (2011). Assessment of MERIS ocean color products using in situ data collected in the Northwestern Black Sea. *IEEE* Proceedings of 5th International Conference on Recent Advances in Space Technologies - RAST2011, 132-136.

Slabakova V., Moncheva S., Slabakova N., Dzhembekova N. (2020) Evaluation of Sentinel3 ocean color products in the Western Black Sea, Proceeding of 1st International conference on ENVIROnmental protection and disaster RISKs (ENVIRORISKs), in press

Suslin, V., Churilova, T., Lee M., Moncheva S. &. Finenko, Z. (2018). Comparison of the Black Sea chlorophyll-a algorithms for SeaWiFS and MODIS instruments. Fundamentalnaya i Prikladnaya Gidrofizika. 11, 3, 64—7.

Suslin, V., & Churilova, T. (2016). The Black Sea regional algorithm of separation of light absorption by phytoplankton and colored detrital matter using ocean color scanner’s bands from 480-560 nm. Int. J. Remote Sens. 37, 4380–4400.

Zibordi, G., Mélin, F., Berthon, J.-F., and Talone, M. (2015). In situ autonomous optical radiometry measurements for Satellite Ocean color validation in the Western Black Sea, Ocean Sci. 11, 275–286.

Suslin, V., Churilova, T., Lee M., Moncheva S. &. Finenko, Z. (2018). Comparison of the Black Sea chlorophyll-a algorithms for SeaWiFS and MODIS instruments. Fundamentalnaya i Prikladnaya Gidrofizika. 11, 3, 64—7.

Suslin, V., & Churilova, T. (2016). The Black Sea regional algorithm of separation of light absorption by phytoplankton and colored detrital matter using ocean color scanner's bands from 480-560 nm. Int. J. Remote Sens. 37, 4380–4400.